Journal of Steroid Biochemistry & Molecular Biology 121 (2010) 124–129

Contents lists available at ScienceDirect

Journal of Steroid Biochemistry and Molecular Biology

journal homepage: www.elsevier.com/locate/jsbmb

Theoretical study of molecular mechanism of binding TRAP220 coactivator to Retinoid X Receptor alpha, activated by 9-cis retinoic acid☆

Mateusz Kurcinski*, Andrzej Kolinski

Department of Chemistry, University of Warsaw, Pasteura 1, 02-093 Warsaw, Poland

ARTICLE INFO

Article history:
Received 9 November 2009
Accepted 26 March 2010

Keywords:
Protein interactions
Flexible docking
Molecular modeling
Nuclear receptors

ABSTRACT

Study on molecular mechanism of conformational reorientation of RXR-alpha ligand binding domain is presented. We employed CABS—a reduced model of protein dynamics to model folding pathways of binding 9-cis retinoic acid to apo-RXR molecule and TRAP220 peptide fragment to the holo form. Based on obtained results we also propose a sequential model of RXR activation by 9-cis retinoic acid and TRAP220 coactivator. Methodology presented here may be used for investigation of binding pathways of other NR/hormone/cofactor sets.

1. Introduction

Nuclear hormone receptors (NR) are ligand-activated transcription factors regulating the expression of target genes [1]. They play widespread and important roles in development, metabolism, homeostasis and disease [2,3]. Retinoid X Receptor (RXR) occupies a central position among other nuclear receptors and plays a crucial role as universal heterodimerization partner for many other members of NR superfamily [4]. Its natural ligand—9-cis retinoic acid activates RXR by binding to a pocket located in RXR's ligand binding domain (LBD). Investigation of crystallographic structures of holo and apo forms of RXR-alpha's LBD show significant structural reorientation of the receptor upon ligand binding. Usually nuclear receptors are investigated in respect of their interaction only with primary ligands [5–7], but they also form complexes with other molecules. In holo-form NRs bind with various cell-specific coactivators, which link receptor with the RNA polymerase II—a gear in transcriptional mechanism, while in apo-form NRs form complexes with co-repressors and act as transcriptional suppressors. Abundance of functions of different nuclear receptors and structural similarity between them at the same time makes the NR class very promising pharmacological target.

2. Materials and methods

Two crystallographic structures of RXR-alpha LBD were analyzed. 1lbd is a structure of monomeric apo form [8] and 1xdk holds the structure of holo-RXR-alpha/holo-RAR-beta heterodimer, liganded by 9-cis retinoic acid and bound to 13 amino acid long peptide—TRAP220 coactivator fragment containing LXXLL motif [9]. RXR residues were divided into four separate classes: ligand active site, cofactor active site, structurally conserved residues and others (Fig. 1). Residue was marked as ligand active site if any of its heavy atoms was located within 4.5 Å radius from any of ligand's heavy atoms. Analogues procedure was used to find cofactor active site. Global distance test (GDT) was calculated on 1lbd and 1xdk structures to find fragments that are highly structurally conserved in both structures. GDT cutoff was set to 0.35 Å in order to match the accuracy of casting the structures to the lattice used in CABS model. Residues previously marked as either ligand or cofactor active site were excluded from the conserved residues set. Table 1 presents comparison between these residue classes.

CABS is a reduced model of protein dynamics and thermodynamics, which proved to be extremely effective in various modeling tasks, such as comparative modeling [10,11], protein fragment reconstruction [12], modeling of folding pathways [13–15] and protein docking [16,17]. CABS stands for Cα(CA), Cβ(B) and united pseudoatom located in the center of mass of the side chain (S), which are the only interaction centers. Positions of Cα atoms are restricted to simple cubic lattice, with spacing equal to 0.61 Å, while remaining atoms are located off the lattice. Sampling is controlled by Replica Exchange Monte Carlo (REMC) scheme [18]. Force field was derived from statistical analysis of regularities found in known protein structures. It consists of generic terms

☆ Special issue selected article from the 14th Vitamin D Workshop held at Brugge, Belgium on October 4–8, 2009.

* Corresponding author. Tel.: +48 22 822 02 11x310; fax: +48 22 822 59 96.
E-mail address: mkurc@chem.uw.edu.pl (M. Kurcinski).

0960-0760/$ – see front matter © 2010 Elsevier Ltd. All rights reserved.
doi:10.1016/j.jsbmb.2010.03.086

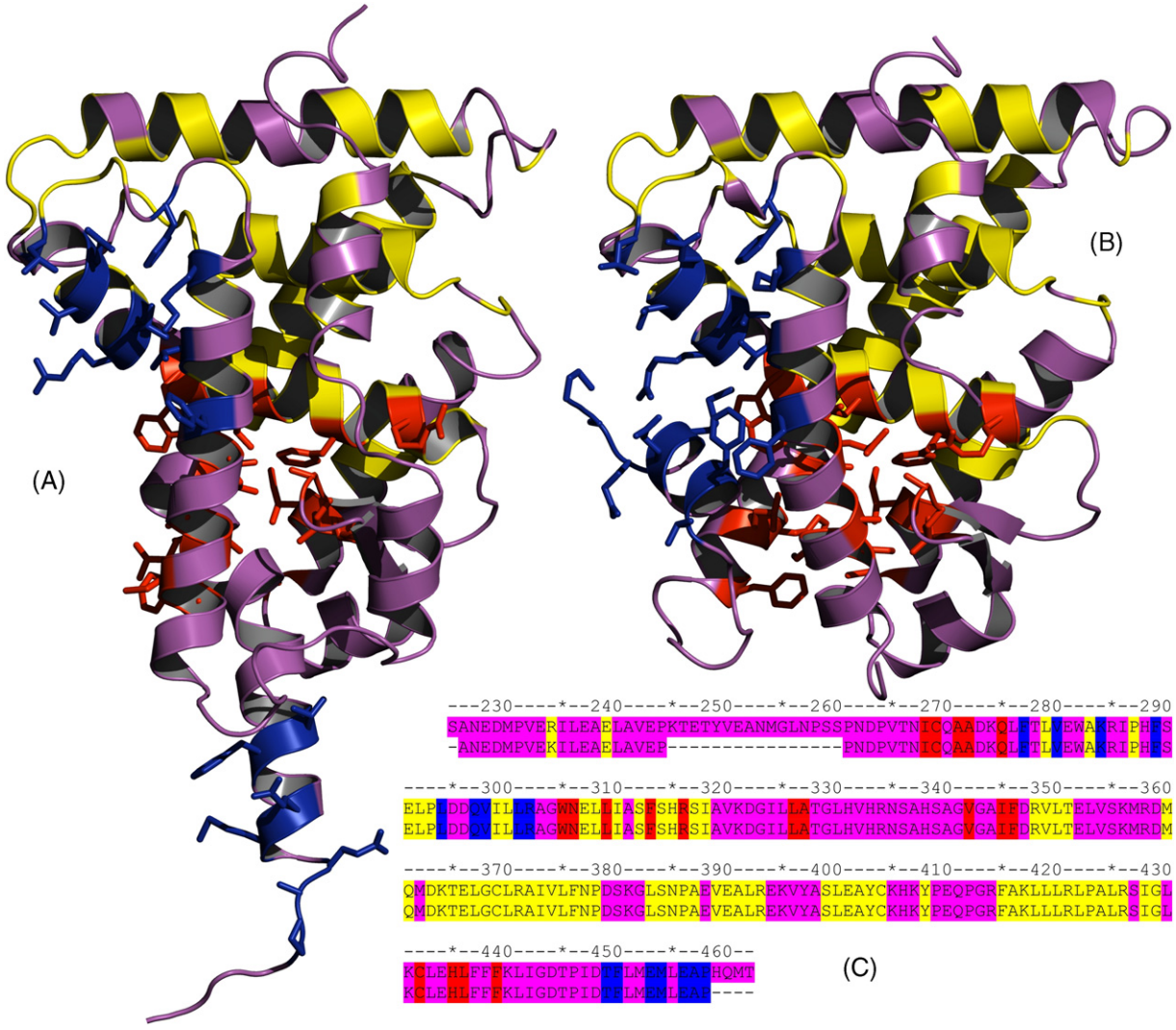

Fig. 1. Crystal structures of RXR-alpha LBD in apo (A) and holo (B) forms. Residues in contact with retinoic acid in apo-RXR are presented in red, those in contact with TRAP220 coactivator in apo-RXR are presented in blue. In yellow most structurally conserved residues (RMSD between apo and holo forms less than 0.35 Å). (C) Alignment of sequences from 1lbd and 1xdk structures, colors as above. (For interpretation of the references to color in this figure legend, the reader is referred to the web version of the article.)

and biases forcing very flexible Cα-trace to behave in protein-like manner and context-dependant pairwise potentials for side chains' interactions. CABS has been fully automated and integrated with user-friendly interface and data processing/analysis tools [19,20] in modeling platform SPMP, commercially available from Selvita Life Sciences Solutions (http://selvita.com) Command-line version of CABS is available for non-commercial users on our website (http://biocomp.chem.uw.edu.pl). Detailed description of the CABS model was presented earlier [21].

CABS was used to model five molecular transformations which RXR molecule does or hypothetically may undergo. In all five cases receptor molecule consisted of residues 225–462 (238 residues) and in all simulations but first (where only structure of the receptor was modeled) cofactor molecule consisted of residues 641–651 (11 residues). Secondary structure was assigned to all residues in the following way: DSSP [22] was run on both 1lbd and 1xdk structures, whenever secondary structure assignment for 1lbd agreed with the one for 1xdk it was also assigned to the modeled residue, otherwise

Table 1
Structural comparison of 1lbd and 1xdk structures.

Residue selection	Number of residues	RMSD	GDT					
			0.5	1.0	2.0	5.0	7.5	10.0
All	217	7.36	0.57	0.81	0.89	0.97	1.00	1.00
Conserved regions	71	0.34	1.00	1.00	1.00	1.00	1.00	1.00
Ligand active site	19	2.97	0.53	0.74	0.84	1.00	1.00	1.00
Cofactor active site	16	14.79	0.56	0.56	0.56	0.56	0.63	0.75
Other	111	6.28	0.28	0.68	0.83	0.97	1.00	1.00

RMSD (root mean square deviation) is defined as square root of averaged distances between corresponding atoms in two sets. GDT (global distance test) is defined as a number of residues in a subset, for which RMSD is below given threshold, divided by total number of residues.

Table 2
Initial conditions in CABS simulations.

Run	Initial structure		Ligand
	Receptor	Cofactor	
I	apo	–	Present
II	holo	Random	Present
III	apo	Random	Present
IV	apo	Random	Absent
V	holo	Native	Absent

secondary structure was set to coil for that residue. All simulations were run with the same force field parameters set, in the same temperature and for the same number of cycles. Brief description of all five runs is presented below.

2.1. Run I (reorientation of the receptor in the presence of the ligand)

Starting structure of the receptor was taken from 1lbd. Conformational flexibility of the residues marked as conserved (Fig. 1) was strongly restricted by a network of distance restraints imposed on Ca atoms. Distances were measured in both 1lbd and 1xdk structures and subsequently averaged. Similarly, residues marked as ligand active site were restrained as well, but this time only distances from 1xdk were used. This was done to indirectly reflect the presence of the ligand in the binding pocket, since CABS is so far capable of handling only protein molecules. Rest of the residues was left unrestrained.

2.2. Run II (cofactor binding to the receptor–ligand complex)

Starting structure of the receptor was taken from 1xdk. Set of distance restraints imposed on the receptor was the same as in the first run. Initial cofactor conformation was random. Moreover the cofactor molecule was shifted away 15 Å from the receptor surface in respect to the 1xdk structure (all cofactor atoms were shifted by a 15 Å—long vector pointing from receptor's center of gravity (COG) to cofactor's COG). No structural restraints were imposed on cofactor structure.

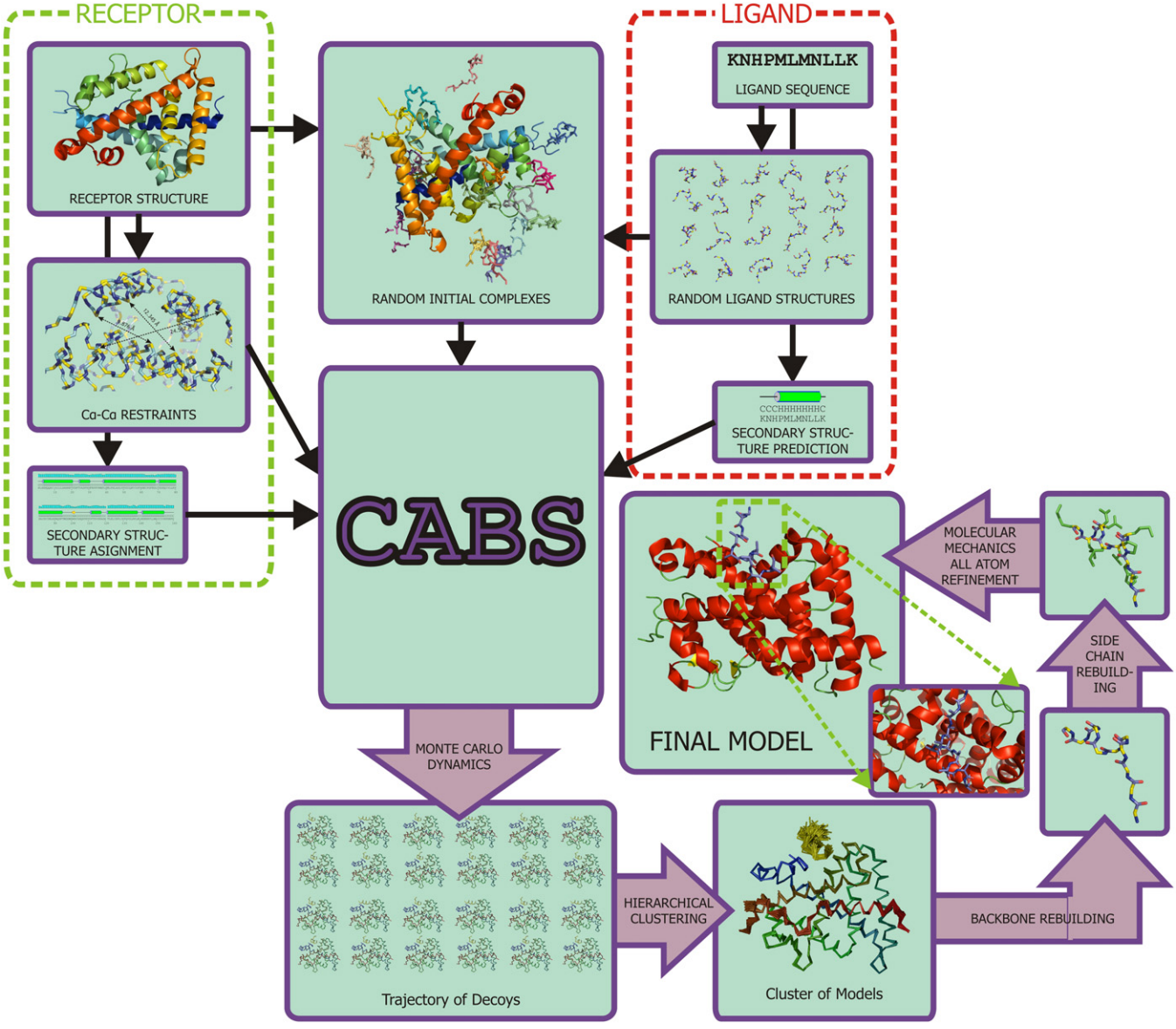

Fig. 2. Modeling scheme used in current work. Complete process is automated and controlled by user-configured scripts.

Table 3
RMSD values calculated on selected models from CABS simulations vs. crystallographic structures of both apo and holo forms of RXR-alpha.

Run	Reference structure	1lbd				1xdk						
	Residue selection	Receptor	Conserved	Ligand active site	Cofactor active site	Receptor	Conserved	Ligand active site	Cofactor active site	Cofactor	Cofactor after receptor superposition	Receptor + cofactor
	Number of residues	217	71	19	16	217	71	19	16	11	11	228
	Top ranked	7.23	0.50	3.00	14.40	0.79	0.36	0.32	1.97	–	–	–
	Best	5.34	0.43	2.83	10.57	0.58	0.31	0.32	0.96	–	–	–
1	Last	7.32	0.50	2.99	14.88	0.78	0.35	0.38	1.83	–	–	–
	Low energy	7.18	0.48	3.04	14.05	0.72	0.35	0.37	1.97	–	–	–
	Average	7.23	0.48	3.01	14.33	0.88	0.35	0.45	2.15	–	–	–
	Top ranked	7.35	0.81	2.97	14.83	0.64	0.71	0.47	0.70	0.95	1.81	0.74
	Best	4.93	0.42	2.81	10.78	0.58	0.29	0.35	0.28	0.73	1.07	0.66
2	Last	7.38	0.80	3.04	14.83	0.64	0.70	0.42	0.63	2.17	2.96	0.91
	Low energy	7.34	0.43	3.00	14.65	0.88	0.31	0.45	1.86	2.75	9.84	2.31
	Average	7.33	0.78	3.01	14.75	0.73	0.69	0.45	0.88	1.62	3.11	0.99
	Top ranked	7.39	0.48	3.07	14.78	0.80	0.33	0.35	1.41	2.17	10.24	2.38
	Best	3.41	0.43	2.14	6.19	0.76	0.31	0.32	1.19	0.69	4.32	1.95
3	Last	7.40	0.48	3.09	14.78	0.81	0.34	0.47	1.41	2.40	10.00	2.34
	Low energy	7.39	0.47	3.09	14.78	0.81	0.34	0.47	1.41	2.40	10.00	2.34
	Average	7.30	0.48	3.02	14.65	0.95	0.35	0.44	1.78	2.57	10.28	2.46
	Top ranked	0.78	0.33	0.23	1.20	7.25	0.42	2.99	14.57	1.67	16.39	7.80
	Best	0.69	0.33	0.23	0.96	6.22	0.40	2.59	14.24	0.75	4.17	6.20
4	Last	0.77	0.33	0.23	1.07	7.24	0.42	2.99	14.56	3.31	13.34	7.51
	Low energy	0.74	0.33	0.23	1.18	7.26	0.42	2.99	14.61	1.77	15.88	7.78
	Average	0.79	0.33	0.24	1.19	7.25	0.42	2.99	14.65	2.86	15.93	7.77
	Top ranked	5.38	0.32	0.28	10.51	4.76	0.42	2.94	7.32	2.32	14.47	5.48
	Best	4.28	0.30	0.19	6.67	3.04	0.40	2.89	1.88	0.80	2.40	3.19
5	Last	7.72	0.30	0.19	15.11	5.20	0.42	2.97	4.16	2.47	10.51	5.61
	Low energy	5.91	0.30	0.19	11.82	5.30	0.42	2.97	6.58	3.60	16.25	6.23
	Average	6.17	0.31	0.26	11.45	5.24	0.42	2.96	6.70	3.24	15.73	6.10

Top ranked, model selected in clustering/refinement procedure; Best, lowest values of listed measures found in all models; Last, last model in CABS trajectory; Low energy, model with the lowest CABS energy; Average, mean value of listed measures, averaged over whole trajectory.

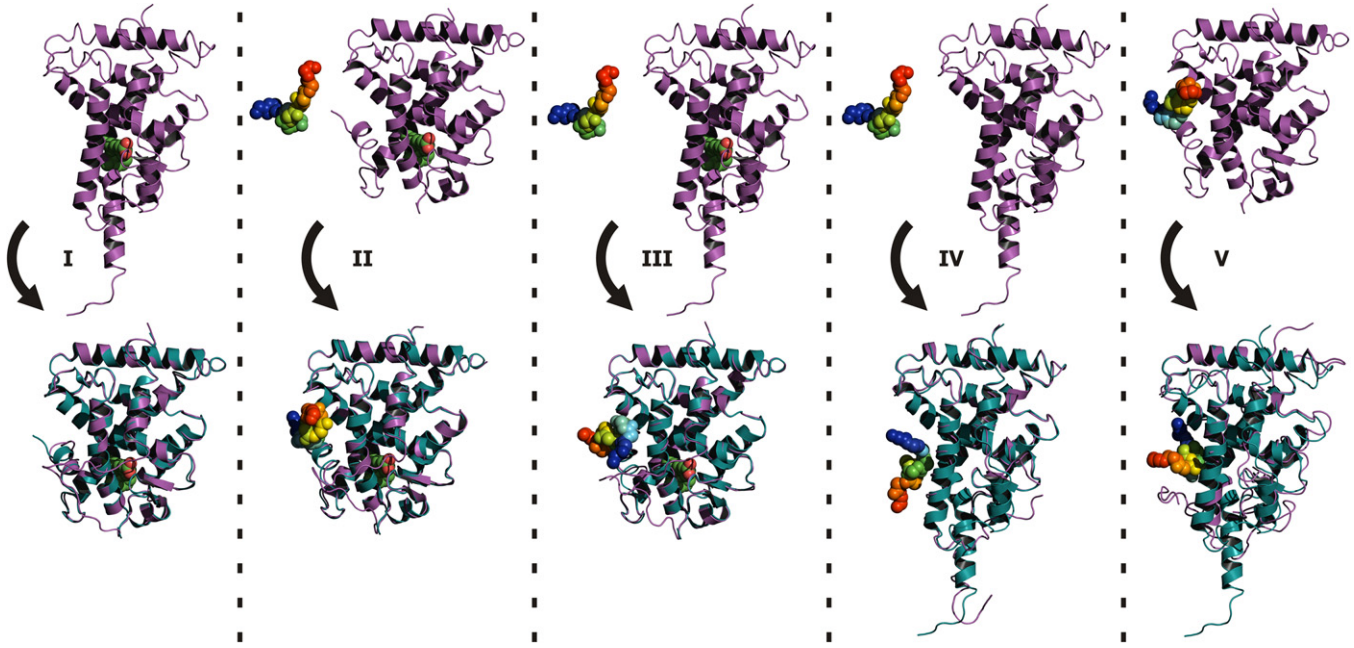

Fig. 3. Initial and final states of the modeled systems in simulations (I–V). In the upper row initial structures of the receptor are shown in purple cartoons. Structure of the cofactor is shown in rainbow spheres. 9-cis retinoic acid—in green. In the bottom row presented are top-ranked models (in purple cartoons (receptor) and rainbow spheres (cofactor)) superposed onto crystallographic structures: 1xdk (I–III) and 1lbd (IV–V). (For interpretation of the references to color in this figure legend, the reader is referred to the web version of the article.)

2.3. Run III (simultaneous reorientation of the receptor in the presence of the ligand and cofactor binding)

Initial structure of the receptor was the same as in the first run and the cofactor structure was the same as in the second run. Identical set of restraints was used as in the first two runs.

2.4. Run IV (cofactor binding to the receptor in apo form)

Initial structures of both receptor and cofactor were the same as in the third run, but distance restraints imposed on active site residues were derived from 1lbd.

2.5. Run V (holo to apo transformation upon ligand dissociation)

Initial structures of both the receptor and the ligand were taken from 1xdk, but distance restraints imposed on active site residues were derived from 1lbd.

Simulation conditions of all five runs are summarized in Table 2. Every run consisted of ten separate iterations differing only by random seed. Every iteration produced 1000 models to sum up to total 10 000 models per run. These models were grouped together by their mutual similarity in two-stage hierarchical clustering procedure [23]—first within 1000 models produced in individual iterations, next medoids of the clusters found in the first stage were clustered again. Medoids of top three biggest clusters were further refined: first reconstructed to all-atom representation using BBQ [24] and SCWRL3.0 [25] and energy-minimized in empirical force field Amber99 [26]. Final model for each run was selected according to the final energy after the minimization [27]. Scheme of the described methodology is presented in Fig. 2.

3. Results and discussion

3.1. Run 1 (reorientation of the receptor in the presence of the ligand)

The process of receptor reorientation was modeled with high accuracy, as confirmed by RMSD between top-ranked model and 1xdk structure in all categories. Cofactor binding site was modeled with 1.97 Å accuracy in respect to the 1xdk structure, which suggests, that additional to ligand-induced conformational adjustment is required upon binding with the cofactor.

3.2. Run 2 (cofactor binding to the receptor–ligand complex)

RMSD between top-ranked model and 1xdk structure calculated on all residues is below 0.8 Å. Additional adjustment in the cofactor binding site is reflected in RMSD decrease to 0.70 Å in that region, when compared to the model obtained in the first run. This suggests that hormone and cofactor activate the receptor sequentially rather than simultaneously.

3.3. Run 3 (simultaneous reorientation of the receptor in the presence of the ligand and cofactor binding)

Although generally low RMSD on the complete structure (2.38 Å), in this run top-ranked model had incorrect orientation of the docked cofactor (RMSD on the cofactor after superposition of the receptor with 1xdk structure was over 10 Å). Furthermore, cofactor itself was in wrong conformation (RMSD 2.17 Å in respect to the 1xdk). The shape of the cofactor binding site was deformed as well (RMSD 1.41 Å). This is another premise suggesting sequential binding of the ligand/cofactor molecules.

3.4. Run 4 (cofactor binding to the receptor in apo form)

In this case receptor remained in its apo form, which inactivated it for cofactor reception as shown by high RMSD values.

3.5. Run 5 (holo to apo transformation upon ligand dissociation)

This case was run to model holo to apo transformation upon ligand dissociation. Indeed shape of both ligand and cofactor active sites has changed significantly. Also cofactor structure and location have been changed. However, apo form was not reconstructed completely—final model shows some structural similarities to both apo and holo forms (RMSD 5.38 Å and 4.76 Å respectively).

In runs I and II the process of binding the ligand and subsequently the cofactor was modeled with great accuracy. At the same time runs III and IV demonstrate that different sequence of binding leads to wrong conformations of final structures. RMSD values are presented in Table 3. Initial and final structures from all simulations are shown in Fig. 3.

4. Conclusions

We present a methodology for investigation of receptor–cofactor binding mechanisms. Case study included prediction of binding TRAP220 coactivator to RXR-alpha receptor in both holo and apo forms, in simultaneous with the ligand, or sequential order. Also ligand-activated apo–holo transformation was investigated. Obtained results remain in agreement with experimental data (crystallographic structures), therefore similar procedure may be applied to investigation of binding pathways in other NR/hormone/cofactor complexes. We also propose a two-stage sequential mechanism of RXR-alpha activation by 9-cis retinoic acid and TRAP220 coactivator, as this matter still remains unresolved. We hope that methodology presented here may find wide spectrum of applications as it provides fast and inexpensive alternative to experimental techniques.

Acknowledgements

This work was supported by the NIH grant no. 1R01GM081680 and Polish Ministry of Science and Higher Education, grant no. NN301465634. Computational part of this work was done using the computer cluster at the Computing Center of Faculty of Chemistry, University of Warsaw. A commercial version of CABS-based modeling software was used (http://www.selvita.com/selvita-protein-modeling-platform.html).

References

[1] R.M. Evans, The steroid and thyroid hormone receptor superfamily, Science 240 (4854) (1988) 889–895.
[2] D.J. Mangelsdorf, et al., The nuclear receptor superfamily: the second decade, Cell 83 (6) (1995) 835–839.
[3] A. Chawla, et al., Nuclear receptors and lipid physiology: opening the X-files, Science 294 (5548) (2001) 1866–1870.
[4] D.J. Mangelsdorf, R.M. Evans, The RXR heterodimers and orphan receptors, Cell 83 (6) (1995) 841–850.
[5] P. Rotkiewicz, et al., Model of three-dimensional structure of vitamin D receptor and its binding mechanism with 1alpha,25-dihydroxyvitamin D(3), Proteins 44 (3) (2001) 188–199.
[6] W. Sicinska, P. Rotkiewicz, H.F. DeLuca, Model of three-dimensional structure of VDR bound with Vitamin D3 analogs substituted at carbon-2, J. Steroid Biochem. Mol. Biol. 89–90 (1–5) (2004) 107–110.
[7] R.R. Sicinski, et al., 2-Ethyl and 2-ethylidene analogues of 1alpha,25-dihydroxy-19-norvitamin D(3): synthesis, conformational analysis, biological activities, and docking to the modeled rVDR ligand binding domain, J. Med. Chem. 45 (16) (2002) 3366–3380.
[8] W. Bourguet, et al., Crystal structure of the ligand-binding domain of the human nuclear receptor RXR-alpha, Nature 375 (6530) (1995) 377–382.
[9] V. Pogenberg, et al., Characterization of the interaction between retinoic acid receptor/retinoid X receptor (RAR/RXR) heterodimers and transcriptional coactivators through structural and fluorescence anisotropy studies, J. Biol. Chem. 280 (2) (2005) 1625–1633.
[10] A. Kolinski, J.M. Bujnicki, Generalized protein structure prediction based on combination of fold-recognition with de novo folding and evaluation of models, Proteins 61 (Suppl. 7) (2005) 84–90.
[11] A. Kolinski, D. Gront, Comparative modeling without implicit sequence alignments, Bioinformatics 23 (19) (2007) 2522–2527.
[12] M. Boniecki, et al., Protein fragment reconstruction using various modeling techniques, J. Comput. Aided Mol. Des. 17 (11) (2003) 725–738.
[13] S. Kmiecik, A. Kolinski, Characterization of protein-folding pathways by reduced-space modeling, Proc. Natl. Acad. Sci. U.S.A. 104 (30) (2007) 12330–12335.
[14] S. Kmiecik, et al., Denatured proteins and early folding intermediates simulated in a reduced conformational space, Acta Biochim. Pol. 53 (1) (2006) 131–144.
[15] S. Kmiecik, A. Kolinski, Folding pathway of the b1 domain of protein G explored by multiscale modeling, Biophys. J. 94 (3) (2008) 726–736.
[16] M. Kurcinski, A. Kolinski, Hierarchical modeling of protein interactions, J. Mol. Model. 13 (6–7) (2007) 691–698.
[17] M. Kurcinski, A. Kolinski, Steps towards flexible docking: modeling of three-dimensional structures of the nuclear receptors bound with peptide ligands mimicking co-activators' sequences, J. Steroid Biochem. Mol. Biol. 103 (3–5) (2007) 357–360.
[18] R.H. Swendsen, J.S. Wang, Replica Monte Carlo simulation of spin glasses, Phys. Rev. Lett. 57 (21) (1986) 2607–2609.
[19] D. Gront, A. Kolinski, Utility library for structural bioinformatics, Bioinformatics 24 (4) (2008) 584–585.
[20] D. Gront, A. Kolinski, BioShell—a package of tools for structural biology computations, Bioinformatics 22 (5) (2006) 621–622.
[21] A. Kolinski, Protein modeling and structure prediction with a reduced representation, Acta Biochim. Pol. 51 (2) (2004) 349–371.
[22] W. Kabsch, C. Sander, Dictionary of protein secondary structure: pattern recognition of hydrogen-bonded and geometrical features, Biopolymers 22 (12) (1983) 2577–2637.
[23] D. Gront, A. Kolinski, HCPM—program for hierarchical clustering of protein models, Bioinformatics 21 (14) (2005) 3179–3180.
[24] D. Gront, S. Kmiecik, A. Kolinski, Backbone building from quadrilaterals: a fast and accurate algorithm for protein backbone reconstruction from alpha carbon coordinates, J. Comput. Chem. 28 (9) (2007) 1593–1597.
[25] M.J. Bower, F.E. Cohen, R.L. Dunbrack Jr., Prediction of protein side-chain rotamers from a backbone-dependent rotamer library: a new homology modeling tool, J. Mol. Biol. 267 (5) (1997) 1268–1282.
[26] E.J. Sorin, V.S. Pande, Exploring the helix-coil transition via all-atom equilibrium ensemble simulations, Biophys. J. 88 (4) (2005) 2472–2493.
[27] S. Kmiecik, D. Gront, A. Kolinski, Towards the high-resolution protein structure prediction. Fast refinement of reduced models with all-atom force field, BMC Struct. Biol. 7 (2007), p. 43.